Phenolic Polymer Solvation in Water and Ethylene Glycol II. Molecular Dynamics Simulations

Eric W. Bucholz, Justin B. Haskins, Joshua D. Monk, Charles W. Bauschlicher, John W. Lawson†

Thermal Protection Materials Branch, NASA Ames Research Center, Moffett Field, CA 94035

Abstract

Interactions between pre-cured phenolic polymer chains and a solvent have a significant impact on the structure and properties of the final post-cured phenolic resin. Developing an understanding of the nature of these interactions is important and will aid in the selection of the proper solvent that will lead to the desired final product. Here, we investigate the role of phenolic chain structure and solvent type on the overall solvation performance of the system through molecular dynamics simulations. Two types of solvents are considered, ethylene glycol (EGL) and H_2O. In addition, three phenolic chain structures were considered including two novolac-type chains with either an ortho-ortho (OON) or ortho-para (OPN) backbone network and a resole-type (RES) chain with an ortho-ortho network. Each system is characterized through structural analysis of the solvation shell and hydrogen bonding environment as well as through quantification of the solvation free energy along with partitioned interaction energies between specific molecular species. The combination of the simulations and analyses indicate that EGL provides a larger solvation free energy than H_2O due to more energetically favorable hydrophilic interactions as well as favorable hydrophobic interactions between CH element groups. In addition, phenolic chain structure significantly impacts solvation performance with OON having limited intermolecular hydrogen bond formations while OPN and RES interact more favorably with the

solvent molecules. The results suggest that a resole-type phenolic chain with an ortho-para network should have the best solvation performance in EGL, H_2O, and other similar solvents.

† Corresponding author: John.W.Lawson@nasa.gov

1. Introduction

Phenolic resins are used in a variety of applications including construction materials [1,2], abrasives [1,3,4], composites [1,5], thermally-insulated foams [1,6], friction materials [1,7–9], and the aerospace industry [1,2]. The wide range of phenolic resin applications is due largely to their relatively low cost and desirable properties such as high mechanical strength, thermal stability, heat resistance, and flame retardancy [1,2,10]. Experimentally, phenolic resins are synthesized through the reaction of phenol with formaldehyde. When the ratio of formaldehyde to phenol in this reaction is greater than unity, a resole-type resin is formed which contains methylol groups substituted on the ortho and para sites of the phenol rings; these ortho and para linking sites are illustrated in Fig. 1a. On the other hand, when the ratio of formaldehyde to phenol is less than unity, the resulting resin is novolac-type which contains significantly fewer of these methylol groups [11]. Unlike novolac resins, the presence of the methylol groups in the resole resins enables them to undergo curing without the addition of a curing agent.

In this work, we consider the fundamental polymer-solvent interactions that are relevant for the processing, and ultimately for the properties, of the phenolic resins. Processing of phenolic resins typically proceeds from low molecular weight oligomers which are subsequently cured in the presence of a solvent. Understanding the chemical details of phenolic interactions with different solvents is of fundamental importance to enable solvent selection for the design of resins with potentially application specific properties. Therefore, we are interested in the behavior and

the interaction of pre-cured phenolic with different solvents. The two considered solvents, ethylene glycol (EGL) and water (H_2O), are commonly used for phenolic processing and are known to provide differing post-cure resins [12,13]. From a fundamental point of view, phenolic is a polar polymer with significant hydrogen bonding opportunities, therefore compatible solvents are expected to be polar as well. The simplest such solvent is of course water whereas EGL is at the next level of molecular complexity with two sites available for hydrogen bonding (H-bonding) as well as possibilities for non-hydrogen bonding interactions.

In particular, we use molecular dynamics (MD) simulations to quantify the phenolic-solvent interaction chemistry. We begin by considering systems with a single phenolic chain solvated in either ethylene glycol or H_2O in order to determine the influence of temperature, solvent type, and phenolic type on the radius of gyration of the phenolic chain. Next, additional MD simulations were performed to evaluate the solvation free energy (SFE) of different phenolic chain types in solution at room temperature. In addition, the relevant controlling molecular interactions were identified and their critical role in solvation dynamics elucidated. Finally, analysis and visualization of the inter- and intramolecular H-bonding within the phenolic chain's solvation shell are reported, further supporting the interpretation of the SFE calculations.

2. Methods

2.1 System and Simulation Details

Three types of phenolic chains were considered in this work, each containing 9 phenol rings, which corresponds to the approximate molecular weight of typical phenolic oligomers. In particular, we consider the following phenolic chain types: an ortho-ortho repeating novolac-type chain (OON), an ortho-para repeating novolac-type chain (OPN), and an ortho-ortho repeating resole-type chain (RES). Each of these phenolic chain types are illustrated in Fig. 1a-c,

respectively. Typical experimentally synthesized phenolic resins are mixtures of ortho-ortho or ortho-para repeat structures; however, using a computational approach, we are able to isolate precisely how the ortho-ortho and ortho-para linking influence the behavior of phenolic chains in solution. Two solvents were considered here, ethylene glycol (EGL) and H_2O. Simulation details for each of the solvated phenolic systems considered are given in Table 1.

Classical MD simulations were performed using the Large-Scale Atomic/Molecular Massively Parallel Simulator (LAMMPS) [14]. All of the MD simulations followed an isothermal-isobaric, or NPT, ensemble where the number of atoms, N, pressure, P, and temperature, T, were kept constant while the total energy and system volume were allowed to fluctuate with time. The interactions for the phenolic chains, both bonded and non-bonded, were evaluated using the all-atom optimized potentials for liquid simulations (OPLS-AA) force field developed by Jorgensen et al. [15]. The bond, angle, and dihedral parameters that were not provided by Jorgensen were obtained from Cornell et al. [16] and from the GROMACS MD package [17]. For EGL, the bonded and non-bonded interactions were taken from the OPLS-AA Scaling Electrostatic Interaction (OPLS-AA-SEI) force field [18], and for H_2O, the TIP3P/ew water model [19] was implemented. Finally, any O-H bonds were constrained using the LAMMPS implemented SHAKE algorithm.

During the solvated phenolic simulations, a time step of 1.0 fs was used, and time integration was performed with the Verlet algorithm. Additionally, the temperature and pressure were controlled by the Nosé-Hoover thermostat [20,21] and barostat [22], respectively. The non-bonded Lennard-Jones and Coulombic interactions were calculated within a 12 Å cutoff, with 1-2 and 1-3 interactions being excluded and 1-4 interactions being weighted by a factor of 0.5. As for the OPLS-AA-SEI force field, the EGL molecules also experienced a weighting factor of 0.8 for 1-5 interactions. Unless otherwise stated, the long-range Coulombic interactions beyond the 12 Å

cutoff were calculated using the PPPM solver with 1E-4 relative accuracy in energy. Each solvated phenolic system was initialized using random velocities and was equilibrated at 298K and 353K for 1 ns. After equilibration, dynamic simulations were carried out for a minimum of 10 ns, but up to 200 ns were performed to ensure that the structural configuration of each phenolic chain was stabilized.

The structural evolution of the phenolic chains was monitored by calculating the radius of gyration (R_g) throughout the simulations. The R_g at each time step was determined by

$$R_g^2 = \frac{1}{M}\sum_n m_n\left(r_n - r_{CoM}\right)^2 \quad (1)$$

where M is the mass of the phenolic chain, r_{CoM} is the center of mass of the phenolic chain, and m_n r_n are the mass and position of atom n, respectively.

For the solvated phenolic systems considered here, H-bonding is an important contributor to the interactions between the phenolic chains and the solvent molecules. From the first peak in the radial distribution function of OH interactions in these systems, we identified three geometric criteria that we implemented to define a h-bond in the simulations: 1) the distance between the oxygen atoms, R_{OO}, must be less than or equal to 3.6 Å; 2) the distance between the hydrogen of the donor hydroxyl and the acceptor oxygen, R_{OH}, must be less than or equal to 2.45 Å; and 3) the angle between the acceptor oxygen, the donor oxygen, and the donated hydrogen ($O_2 \ldots O_1 - H_1$) must be less than or equal to 30°. This is the same criteria used in previous MD simulation studies to define h-bonds between water molecules [23–25]. Analysis of the respective radial distribution functions for OH interactions between EGL/H_2O and each phenolic chain type indicated that this same geometric criteria could be used to define all h-bonds considered in this work.

2.2 Solvation Free Energy

The solvation free energy, ΔG_{solv}, may be used to gauge the relative solubility of a polymer in different solvents. In this work, ΔG_{solv} represents the free energy change of transitioning reference polymer (P) and solvent (S) systems into a combined system where the polymer is solvated (P+S). Specifically, P represents a gas-phase polymer chain while S is a liquid-phase solvent. To obtain ΔG_{solv} from MD simulation, the potential energies of both the reference systems as well as the combined system must be unified into a single expression through a continuous set of state variables, Λ. The continuity of potential energy in Λ, $U(\Lambda)$, enables the evaluation of ΔG_{solv} via thermodynamic integration,

$$\Delta G_{solv} = \int_{\Lambda^{P,S}}^{\Lambda^{P+S}} \left\langle \frac{\delta U(\Lambda)}{\delta \Lambda} \right\rangle_{\Lambda} d\Lambda \tag{2}$$

where $\langle ... \rangle_{\Lambda}$ denotes the ensemble average of a system at a fixed Λ.

A commonly employed [26] Λ-dependent potential energy suitable for thermodynamic integration is

$$U(\Lambda) = U^{P} + U^{S} + U^{P+S}(\Lambda) \tag{3}$$

where U^{P} is the self-energy of the polymer, U^{S} is the self-energy of the solvent molecules as well as the solvent-solvent interaction energy, and U^{P+S} is the interaction energy of the polymer with the solvent. The Λ-dependence is localized to the polymer-solvent interaction terms. The convention followed in this work is that $\Lambda = 0$ removes U^{P+S} and corresponds to the separate P and S systems, while $\Lambda = 1$ fully enforces U^{P+S} and corresponds to the P+S system. As such, the polymer-solvent interactions can be constructed as

$$U^{P+S}(\Lambda)=\sum_{i,i<j}\left[\lambda_{RD}U_{RD}^{P+S}\left(r_{ij},\lambda_{RD}\right)+\lambda_{ES}U_{ES}^{P+S}\left(r_{ij}\right)\right] \quad (4)$$

where U_{RD}^{P+S} is the repulsive-dispersive energy, U_{ES}^{P+S} is the local and long-range electrostatic energy, r_{ij} is the distance between particles *i* and *j*, λ_{RD} governs the repulsive-dispersive interactions, and λ_{ES} governs the electrostatic interactions, with Λ being composed of the set $\{\lambda_{RD},\lambda_{ES}\}$.

In practice, the evaluation of ΔG_{solv} is performed in a two-step process. The first step is the evaluation of $\int_0^1\langle\partial U(\Lambda)/\ \partial\lambda_{RD}\rangle_{RD}\,d\lambda_{RD}$ while keeping $\lambda_{ES}=0$. The second step is the evaluation of $\int_0^1\langle\partial U(\Lambda)/\ \partial\lambda_{ES}\rangle_{ES}\,d\lambda_{ES}$ while keeping $\lambda_{RD}=1$. The sum of the two-step integration process yields ΔG_{solv}. The repulsive-dispersive interactions of concern during the first integration are represented through a soft-core Lennard-Jones potential [27],

$$U_{RD}^{P+S}\left(r_{ij},\lambda_{RD}\right)=4\varepsilon_{ij}\left[\left(\frac{\sigma_{ij}^6}{\alpha(1-\lambda_{RD})^2\sigma_{ij}^6+r_{ij}^6}\right)^2-\frac{\sigma_{ij}^6}{\alpha(1-\lambda_{RD})^2\sigma_{ij}^6+r_{ij}^6}\right] \quad (5)$$

where σ and ε are the standard Lennard-Jones 12-6 potential parameters and α (set to 0.5 in the simulations performed here) determines the energy as $r_{ij}\to 0$. The soft-core Lennard-Jones potential removes the possibility of having energetic singularities at small values of λ_{RD}, where the interaction between particles is small and r_{ij} may approach zero. The soft-core energy reduces to that of the standard Lennard-Jones 12-6 energy for $\lambda_{RD}=1$. Because U_{RD}^{P+S} is fully in play during the second integration over λ_{ES}, there is no potential for core overlap. As such, no soft-core treatment is needed, and standard electrostatic interaction may be employed.

2.3 Energy Partitioning

In order to identify contributions from different, specific molecular interactions within the solvated phenolic systems, a modified version of LAMMPS was employed to partition the interaction energies into sums between specified atom types. For the purposes of energy partitioning, separate simulations for each of the following three systems were performed: a solvated phenolic system, an isolated solvent system, and an isolated phenolic system. For each simulation, the total average internal energy was decomposed into bonded and non-bonded contributions for solvent/solvent interactions (S-S), phenolic self-interactions (P-P) and solvent/phenolic interactions (S-P). The interactions were further decomposed into contributions between specific molecular units, in particular OH and CH, on the polymer chains and the considered solvents. This partitioning permitted examination of the individual interactions between solvent/solvent, phenolic/phenolic, and solvent/phenolic atoms but also allowed for the identification of hydrophobic/hydrophobic, hydrophobic/hydrophilic, and hydrophilic/hydrophilic contributions.

Note that in this paper, we use the terms “hydrophobic” and “hydrophilic” more generally to refer to positive polymer-solvent interactions that either involved H-bonding (hydrophilic) or do not involve H-bonding (hydrophobic). Therefore, positive interactions of water with phenolic will always be hydrophilic via h-bonding between the water and the phenolic hydroxyl groups. However, EGL can have both H-bonded and non-H-bonded interactions.

Combining solvation free energies with energy partitioning permits calculation of additional thermodynamic quantities from the relationship

$$\Delta G_{solv} = \Delta E_{solv} - T\Delta S_{solv} \tag{6}$$

where T is the system temperature and ΔS_{solv} is the change in entropy during to solvation. ΔE_{solv} represents the change in total internal energy due solvation determined by

$$\Delta E_{solv} = E^{P+S} - (E^{P} + E^{S}) \tag{7}$$

which can be decomposed into solvent and polymer components

$$\Delta E_{solv} = (E_{S-S}^{P+S} + E_{P-S}^{P+S} + E_{P-P}^{P+S}) - (E_{P-P}^{P} + E_{S-S}^{S}) \tag{8}$$

where the superscripts indicate the system and the subscripts gives the partition. Further decomposing into bonded (*b*) and non-bonded interactions (*nb*) yields

$$\Delta E_{solv} = \Delta E_{nb,S-S} + \Delta E_{nb,P-P} + E_{nb,S-P}^{P+S} + \left(E_{b}^{P+S} - E_{b}^{P} - E_{b}^{S}\right) \tag{9}$$

where $\Delta E_{nb,S-S} = E_{nb,S-S}^{P+S} - E_{nb,S-S}^{S}$ and $\Delta E_{nb,P-P} = E_{nb,P-P}^{P+S} - E_{nb,P-P}^{P}$. The terms E_{b}^{P+S}, E_{b}^{P}, and E_{b}^{S} refer to the bond energies in the solvated phenolic system, the isolated phenolic system, and the isolated solvent system respectively. The change in entropy due to solvation can be extracted from these expressions immediately.

3. Results

3.1 Radius of Gyration

The R_g for each 9-ring phenolic chain type and for the 27-ring OON chain is illustrated in Fig. 2. The R_g of each phenolic chain is largely independent of the solvents and temperatures considered in this work. Specifically, the R_g is consistent with a collapsed oligomer architecture similar to the structures previously shown in Fig. 1; it was also noted that the 27-ring OON chain showed the same preferential collapsed structure under the conditions considered. Although the phenolic chains took considerably longer to transition to their equilibrated structure in EGL compared to H_2O, this is likely a result of the larger self-diffusivity for water compared to EGL. Due to the similar molecular structure of the phenolic chains in EGL and H_2O, more detailed investigation is needed to understand how the different phenolic types interact with each solvent.

It is important to note that frequently R_g is used as a diagnostic to distinguish "good" vs "bad" solvents, i.e. good solvents have larger R_g indicating more favorable polymer-solvent interactions while "bad" solvents exhibit the converse. Our results suggest however that for our system, R_g does not have sufficient sensitivity to distinguish the relative value of our solvents and, therefore, more detailed investigation is required. In order to quantify these differences, the free energy of solvation was computed as a function of phenolic type and solvent type.

3.2 Solvation Free Energy

Solvation free energies as well as energy partitioning results for the three phenolic chain types (OON, OPN, RES) and the two solvents (H_2O, EGL) are provided in Table 2. Results are for 9-ring chains at 298K. Columns 3-5 give the free energy, the internal energy and the entropy of solvation. Columns 6-8 give the *non-bonded,* internal energy change due to interactions between the polymer (P) or solvent (S) subsystems as described in Section 2.3. Change in energy values for $S-S$, $P-P$, and $S-P$ interactions refer only to the non-bonded interaction energies; the relevant bonded interaction energies, although not explicitly provided, are accounted for in ΔE_{solv} in the manner detailed in Eq. 9. Independent of solvent type, the solvation free energy is highest for the RES chain and lowest for the OON chain. This is due to the presence of the 11 methylol groups attached to the phenolic rings in the resole chain that are absent from the novolac chains. In addition, the solvation free energy for OPN is higher than that for OON. This is due to the larger number of intramolecular h-bonds, which limits the OONs ability to form intermolecular h-bonds with the solvent molecules. The approximately 40 kcal/mol energy difference between OPN and OON for ΔE_{S-P} supports this explanation; however, additional energy partitioning analysis will be required in order to fully confirm or refute this claim.

Due to the transition of a phenolic solute from the gas phase to a liquid phase, the entropy change for the solvation process is negative for all systems. Gas phase polymer molecules typically have larger entropy than their solvated counterparts. This is in part due to solvent-induced constraints on the polymer that reduce the configurational entropy. Additionally, the arrangement of strongly interacting solvent molecules in the solvation shell of the polymer is another ordering effect that reduces entropy. Comparatively, the OON chains exhibit the largest entropy, which may be attributed to the strong internal H-bonding that severely restricts the polymer configurational space, regardless of solvation effects, and the lack of external OH sites to strongly interact with the solvent.

More detailed energy partitioning analysis is presented for solvent/phenolic interactions as well as pure phenolic interactions in Tables 3, 4 and 5. Negative/positive energy values refer to attractive/repulsive interactions, respectively. Table 3 shows that the non-bonded interaction energy between solvent OHs and solute OHs increases significantly for both EGL and H_2O as the chain type changes from OON to OPN to RES. This is consistent with the expectation of increasing opportunities for H-bonding between these chain types. Table 4 shows the interaction energies between the entire solute chains and specific solvent element groups as well as between the entire solvent molecules and specific solute element groups. This provides a clear summary of the overall differences in interaction energy between the different phenolic chains considered here.

Table 5 shows the effect of solvation on the energies for the phenolic chains. One non-trivial effect is the change of a negative OH-OH interaction energy to a positive OH-OH interaction energy for OON and OPN, respectively. This again indicates that the OON structure favors intramolecular H-bonding while the OPN, and also the RES, structure provides more opportunities for intermolecular h-bonds to form with the solvent molecules.

Comparing phenolic solvation differences between EGL and H_2O, Table 2 shows that the solvation free energy in EGL is higher than in H_2O for each respective system. To better understand the source of the solvation energy differences between EGL and H_2O, we will refer again to the detailed breakdown of the energy partitioning analyses provided in Tables 3 – 5. Table 3 shows that EGL has significantly larger attractive interaction energies than H_2O between the phenolic OHs and solvent OHs. These results also indicate that there is a strong attractive interaction energy between the EGL CHs and the phenolic CHs, which is obviously a type of non-bonded interaction that is unavailable to H_2O. Alternatively, for H_2O, the interaction between OHs and solute CHs is attractive, whereas the OH to CH interactions between solute and solvent molecules are strongly repulsive in EGL systems. In order to better highlight how the solvation free energy is larger in EGL systems than for H_2O despite the large repulsive OH to CH interactions, **Table 4** combines the previous results to show interaction energies between entire solvent molecules and specific phenolic element groups as well as between entire polymer chains and specific solvent element groups. By combining these interaction energies, the phenolic chains are seen to interact more favorably with EGL OHs than with H_2O while the interaction energies between the solvent molecules and the phenolic OHs are comparable between EGL and H_2O. The factor that makes the difference for why EGL provides a higher solvation free energy is due to the interaction energies between EGL and the phenolic CHs, which are considerably stronger than for H_2O. This difference is even more pronounced for the RES chains which indicate an attractive non-bonded interaction energy with the EGL CHs, whereas the same interactions for OON and OPN are repulsive. Table 5 energy partitioning analysis for intramolecular phenolic chain interactions shows that both EGL and H_2O perform similarly with the non-bonded interaction

energies being, in general, more positive in the solvated systems than for the isolated phenolic chains in vacuum.

3.3 Solvation Shell Structure

We analyzed the solvation shell structure for each solvent and each phenolic chain type throughout the dynamic simulations. For this analysis, the solvation shell is defined as the solvent molecules that are located within the first peak of respective radial distribution functions of intermolecular distances between phenolic atoms and the centers of mass of the solvent molecules. Fig. 3a and 3b give an illustration of the OPN chain solvated in EGL and H_2O, respectively, where intermolecular h-bonds are denoted in red. As can be clearly observed, the solvation shells are made up of numerous solvent molecules that exhibit both h-bonded and non-h-bonded interactions with the phenolic chain. It is further evident from Fig. 3 that significantly more solvent molecules interact with the phenolic chains via non-h-bonded interactions than h-bonded interactions, which supports the demonstrated importance of hydrophobic interactions discussed in the previous section. Specifically, OPN and RES chains are expected to interact more strongly with the solvents than OON due to the increased potential for intramolecular h-bond formation. Qualitatively, no significant solvation differences were observed between the two solvents.

A more quantitative analysis of the solvation shell structures was developed as depicted in Figure 4. In this binary analysis, a specific solvent/solute interaction is labelled either 1 or 0 depending on whether that interaction is present or not. The three individual solvation interactions included in this analysis are**:** Fig. 4a) solvent molecule and phenolic hydroxyl, labelled [100]; Fig. 4b) solvent molecule and center of phenolic ring, labelled [010]; and Fig. 4c**)** solvent molecule and phenolic methylene linker, labelled [001]. It is important to note that any combination of these

three separate solvation interactions are possible, i.e. [110] indicates that a solvent molecule interacts with both a phenolic hydroxyl and the center of a phenolic ring.

Two criteria were used to determine whether the binary indicators for a specific interaction would be toggled as 1 (on) or 0 (off). The first is an interaction distance criteria which is 3.5 Å for [100], 4.2 Å for [010], and 4.2 Å for [001]. The second is a persistence criteria meaning that the previous distance criteria must be met for at least two consecutive MD trajectory outputs or 20 ps of simulation time. The results of this binary analysis are provided in Figure 5 which shows the average number of solvent/phenolic interactions at any given point during the solvation simulations. The persistence criteria was used to identify more stable interactions. Here, all possible combinations of the binary naming scheme from Figure 4 are represented for interactions between the three different phenolic chains and EGL. Likewise, since H_2O does not contain hydrophobic species, only interactions between phenolic hydroxyls and H_2O molecules, or [100] types, are considered as can be seen in the inset in Figure 5.

For interactions between EGL and OON, it is evident that the most prevalent interaction types are between hydrophobic species, specifically the [010] and [001] types. Few interactions of the type [100] were observed due to the extent of intramolecular OON h-bonds discussed in the previous section. As for OPN and RES, the [100] type is the preferential interaction for EGL molecules due to the lack of intramolecular H-bonding in OPN and the presence of additional hydrophilic species within the methylol units along the RES chain. Considerably fewer hydrophobic interaction types were observed between EGL and either OPN or RES chains. Regarding the two- and three-component interaction types, i.e. [110], [101], [011], and [111], relatively few of each were observed between EGL and any of the chain types considered here; this is due to the fact that multiple distance and persistence criteria must be met simultaneously

which reduces the likelihood that such interactions will be found. As is shown within the inset in Figure 5, H_2O follows the same trend observed for EGL with the average number of [100] type interactions increasing from OON to OPN to RES.

3.4 Hydrogen Bonding

An important attribute of the solvation shell, and ultimately of the performance of the solvent itself, is H-bonding between the solvent molecules and the hydroxyl units of the phenolic chains. For analysis of the H-bonding occurring in the solvated phenolic simulations, we quantify the amount of H-bonding that is present at any given time as well as the relative lifetimes of the different types of H-bonds that can be formed in these solvated phenolic systems. Using the geometric criteria for defining h-bonds previously discussed in Section 2.1, Tables 6 and 7 indicate the average number of h-bonds that are present for each phenolic chain type at 298 and 353K in EGL and H_2O, respectively. Specifically, three different types of h-bonds are reported ("P to S," "S to P," and "P to P"). The naming scheme is such that a h-bond of type "P to S" indicates an oxygen within the phenolic hydroxyl is the h-bond donor while an oxygen within the solvent molecule is the h-bond acceptor. The "P to P" h-bonds indicate intramolecular bonding within the phenolic chains. From these tables, it is evident that the OON chains exhibit substantial intramolecular H-bonding, as was previously noted in Section 3.2. As is shown in the data, the RES chain has nearly the same amount of "P to P" h-bonds as OON since its base conformation is also ortho-ortho. Also, it is observed that the structural change from OON to OPN results in the loss of essentially all of the intramolecular h-bonds.

For "P to S" and "P to P" type h-bonds, both EGL and H_2O result in similar average numbers of h-bonds. The lack of "P to P" h-bonds in OPN relative to OON results in significantly more "P to S" h-bonds, which is due to OPN's hydroxyls being available to function as

intermolecular h-bond donors. As for "S to P" type h-bonds, the analysis shows that more h-bonds form between the different phenolic chains and H_2O than EGL. This observation results from the ability of multiple H_2O molecules to form h-bonds with the same phenolic hydroxyl. Finally, regarding RES, despite having the same ortho-ortho conformation as OON, RES still has large amounts of intermolecular H-bonding due to the presence of methylol groups attached to each phenol ring.

In order to determine the stability and average lifetimes of h-bonds within each of the solvated phenolic systems, a time-dependent autocorrelation function was implemented of the form [25,28],

$$C_{c,i}(t) = \left\langle \frac{\sum_{i,j}^{n} S_{ij}(t+t_0) \cdot S_{ij}(t_0)}{\sum_{i,j}^{n} S_{ij}(t_0)} \right\rangle$$

(10)

where *n* is the number of hydroxyls in the system, *ij* is a potential h-bond pair being analyzed, t_0 is the initial time, and S_{ij} is the h-bond occupation number which is defined to be *1* if the *ij* pair is h-bonded or *0* if they are not. The subscript C_c refers to a continuous autocorrelation function where any h-bond that exists as $S_{ij}(t_0) = 1$ is only allowed one transition from *1* to *0*; this means that the first time, $t + t_0$, a h-bond between atoms *i* and *j* is broken, $S_{ij}(t + t_0)$ will be set to *0* and is never allowed to be set to *1* again. The other subscript C_i refers to an intermittent autocorrelation function. Unlike the continuous definition, with the intermittent definition, $S_{ij}(t + t_0)$ is permitted to transition freely between *1* and *0* for all times $t + t_0$.

Using the intermittent autocorrelation function, the stability of the three types of h-bonds at 298K within the solvated systems are illustrated for OON in Fig. 6a-b, OPN in Fig. 6c-d, and RES in Fig. 6e-f. In addition, solvated EGL and H_2O systems are represented in Fig. 6a, c, e and Fig. 6b, d, f, respectively. As can be seen, intramolecular "P to P" h-bonds within OON and RES are mostly constant and long lived, while they decay quickly within OPN. The two intermolecular h-bond types, "P to S" and "S to P," decay much faster in H_2O than is observed in EGL. It is also observed that "P to S" type h-bonds generally decay slower in both H_2O and EGL than "S to P" type h-bonds. The observed asymmetry between "P to S" and "S to P" type h-bonds is likely due to differences in the partial charges of each hydroxyl type in the solvated systems. For intermolecular h-bonds involving OPN and OON chains, the partial charge difference is greater when the phenol hydroxyl is the h-bond donor than when it is the h-bond acceptor, which leads to increased stability of "P to S" type h-bonds. For RES, on the other hand, the partial charge differences are less pronounced when the methylol hydroxyls act as either the h-bond donor or acceptor; this leads to a reduced asymmetry between "P to S" and "S to P" type h-bonds for RES because the intermolecular h-bonds primarily involve methylol groups while the phenol hydroxyls mostly form intramolecular h-bonds.

The results from Fig. 6 suggest that h-bonds between EGL and the phenolic chains are more stable than those between H_2O and phenolic, potentially resulting from the smaller diffusion coefficient of EGL. The results also indicate that intramolecular h-bonds within an ortho-ortho structure demonstrate the highest stability which suggests that the overall solvation quality of phenolic chains in any appropriate solvent will be affected by the structure of the phenolic chains themselves. However, the use of a resole-type phenolic structure can be used to increase the interaction with the solvent.

In order to better quantify h-bond stability in the solvated systems, the average h-bond residence times were calculated from the continuous autocorrelation function, C_c. An exponential decay function of the form,

$$C_c = A_1 \exp\left[\frac{-t_{ins}}{t_1}\right] + A_2 \exp\left[\frac{-t_{ins}}{t_2}\right], \quad (11)$$

is fit to data similar to that shown in Fig. 6, where t_{ins} is the instantaneous simulation time relative to t_0, and A_1, A_2, t_1, and t_2 are the fitting factors. From each fitting curve, the average h-bond residence time is defined as,

$$t_{res} = \frac{A_1 \cdot t_1 + A_2 \cdot t_2}{t_1 + t_2}. \quad (12)$$

The results of this analysis for each chain type at 298 and 353K are summarized in Tables 8 and 9 for EGL and H_2O, respectively. As is expected, the average h-bond residence time decreases as temperature increases for all chain types and solvent combinations considered here. Also noted is that the "P to P" residence times for the ortho-ortho type OON and RES chains are significantly longer than those of the OPN chains. Likewise, the transition from OON to OPN results in approximately a 60% increase in the residence time of "P to S" h-bonds, resulting from the OPN's increased capacity to form intermolecular h-bonds. The data further indicates that the presence of the methylol units on the RES chains results in intermolecular "P to S" and "S to P" type h-bonds consistent with those observed within the solvated OPN systems while also having the same long-lasting intramolecular "P to P" h-bonds found in the solvated OON systems. Finally, for almost all analyses performed here, the average h-bond residence times for all three h-bond types decrease significantly, ranging between 18 and 92%, for the varied phenolic chains in H_2O compared to EGL.

3.5 Diffusivity

Phenolic chains dynamics in solution for each solvent were analyzed by considering the average mean square displacement (MSD). MSDs for chains solvated in EGL are shown in Fig. 7a, c, e and in H_2O in Fig. 7,b, d, f. OON, OPN, and RES chains are provided in Fig. 7a, b, Fig. 7c, d, and Fig. 7e, f, respectively. Each of these simulations was carried out for 40 ns with mean square displacement analyses performed every 10 ps. As is evident from Fig. 7, temperature has a more significant influence on the mobility of each chain type in EGL than in H_2O with a temperature increase from 298K to 353K resulting in a higher percentage increase in mean square displacement in EGL. Also, it can be seen that, independent of temperature, the phenolic chains displace faster in H_2O than in the corresponding EGL systems.

Quantification of the diffusivity differences in these solvated phenolic systems was done by calculating the diffusion coefficients as a function of time using the Einstein relation [29]

$$D = \lim_{t\to\infty} \frac{\left\langle \left| \vec{r}_n(t) - \vec{r}_n(0) \right|^2 \right\rangle}{6t} \tag{13}$$

where $\vec{r}_n(0)$ and $\vec{r}_n(t)$ are the initial position and the position at time, *t*, for atom *n*. Table 10 provides a summary of the diffusion coefficients for each of the solvated 9-ring phenolic chain systems; the values provided are averages for the final 5 ns of the total 40 ns simulation time along with the standard deviations for each analysis. From Table 10, it is observed that a temperature increase from 298K to 353K for the solvated EGL systems results in a phenolic chain diffusivity increase of about an order of magnitude for OPN and RES chains as well as an increase of approximately three times for OON. Likewise, the phenolic chain diffusivity in H_2O is significantly greater than in the respective EGL systems. However, the data suggests that the phenolic chain type has no significant influence on its diffusivity in either EGL or H_2O.

4. Discussion

From a conformational perspective, the three types of phenolic chains considered here do not qualitatively differ when solvated in either EGL or H_2O as is evidenced by the collapsed oligomer structure that is illustrated in Fig. 1 and from the R_g provided in Fig. 2. This indicates that the solvation differences between EGL and H_2O must result from differences in the local h-bonding environment as well as intermolecular interactions present within each phenolic chain's solvation shell. Through structural analysis of the solvation shell, differences between the OON, OPN, and RES type phenolic chains are observed, as demonstrated in Fig. 5. These observations suggest that the OON chain interacts with EGL primarily through [010] and [001] type hydrophobic interactions whereas OPN and RES preferentially interact through [100] type hydrophilic interactions. However, OPN and RES also yield [010] and [001] type hydrophobic interactions similar to those observed for OON but to a lesser degree. In addition, analysis of H_2O solvated systems yields the same observations with the numbers of hydrophilic [100] type interactions increasing from OON to OPN to RES type phenolic chains. Analysis of the H-bonding environment within each solvated phenolic system, detailed in Tables 6 and 7, provides support for the solvation shell observations showing that OON has relatively few intermolecular h-bonds with either solvent while OPN and RES have significantly more.

Ultimately, calculations of the solvation free energy of each type of phenolic chain along with the partitioning of the interaction energies between different molecular species is needed in order to fully understand the solvation differences between EGL and H_2O for pre-cured phenolic polymers. Table 2 indicates that each respective phenolic chain has a higher solvation free energy in EGL than in H_2O with RES possessing the highest solvation free energy followed by OPN and OON in that order. From the energy partitioning analysis provided in Table 4, it is shown that interactions between solute molecules and solvent OHs are more energetically favorable for EGL

than for H_2O. Furthermore, the phenolic systems solvated in EGL have additional favorable interactions between the solvent chains and the solute CHs which leads to additional improved solvation performance. Finally, as for differences between EGL and H_2O with regard to the H-bonding environment, analysis of the h-bond residence times provided in Fig. 6 and Tables 8 and 9 show that intermolecular "P to S" and "S to P" type h-bonds indicates that these h-bonds have substantially longer lifetimes in EGL than in H_2O. The longer residence times of the h-bonds in EGL allow for longer-lasting, energetically favorable hydrophilic interactions. Finally, the simulations and analyses performed here indicate that there is a significant structural dependence on the overall solvation performance in either EGL or H_2O. Specifically, the ortho-ortho network within the novolac-type OON chain leads to increased intramolecular h-bonds which limits the ability for intermolecular h-bonds to form effectively reducing solvation capabilities. The presence of either an ortho-para network or a resole structure functions to negate these effects. Thus, our work suggests that the best solvation properties in EGL and H_2O and likely other similar solvents would be obtained through the use of resole-type pre-cured phenolic polymer having a primarily ortho-para conformation.

Conclusions

The simulations and analyses presented here indicate pre-cured linear phenolic chains of both novolac- and resole-type and having either ortho-ortho or ortho-para network structure have a collapsed oligomer structure in EGL and H_2O at temperatures between 298 and 353K. Despite the qualitative similarities between these systems, analysis of the solvation free energy shows that phenolic chains in EGL yield a larger solvation free energy than in H_2O. Through an energy partitioning analysis of the interaction energies between specific molecular species, we demonstrate that the larger solvation free energies in EGL results from more energetically

favorable interactions between hydrophilic species combined with favorable interactions between the EGL molecules and the hydrophobic CH groups along the phenolic chain.

Thorough analysis of these solvated phenolic systems further indicates that the structure of the phenolic chains themselves has a significant influence on the solvation energy regardless of solvent type. Specifically, the OON type chain has the lowest solvation free energy due to preferential interactions with its solvation shell via its hydrophobic components; this results from an abundance of intramolecular H-bonding permitted by the ortho-ortho chain conformation. Although the OPN type chain has similar hydrophobic interactions, the ortho-para chain conformation limits the ability to form intramolecular h-bonds allowing for numerous intermolecular h-bonds to form with the solvent which raises the solvation free energy. The RES type chain had the larger solvation free energy of the chains considered because of the presence of 11 methylol groups attached to the phenol rings; therefore, despite having an ortho-ortho conformation similar to OON, the methylol groups increase RES's capacity to form intermolecular h-bonds with the solvent molecules. From these results, solvation problems that may occur during phenolic polymer processing could be alleviated with the use of phenolic chains possessing either a primarily ortho-para backbone structure or that are resole-type. As such, we speculate that the best solvation performance would be realized through the use of an ortho-para resole-type pre-cured phenolic polymer.

References

[1] L. Pilato, Phenolic Resins: A Century of Progress, Springer-Verlag, Berlin, 2010.

[2] C.P.R. Nair, Prog. Polym. Sci. 29 (2004) 401–498.

[3] J. Kopac, P. Krajnik, J. Mater. Process. Technol. 175 (2006) 278–284.

[4] B. Strzemiecka, A. Voelkel, D. Chmielewska, T. Sterzyński, Int. J. Adhes. Adhes. 51 (2014) 81–86.

[5] B.K. Kandola, E. Kandare, in:, A.R. Horrocks, D. Price (Eds.), Adv. Fire Retard. Mater., Woodhead Publishing, Cambridge, UK, 2008, pp. 398–442.

[6] H. Shen, S. Nutt, Compos. Part A Appl. Sci. Manuf. 34 (2003) 899–906.

[7] W. Österle, M. Griepentrog, T. Gross, I. Urban, Wear 251 (2001) 1469–1476.

[8] Y. Lu, C.F. Tang, M.A. Wright, J. Appl. Polym. Sci. 84 (2002) 2498–2504.

[9] J. Yu, J. He, C. Ya, J. Appl. Polym. Sci. 119 (2011) 275–281.

[10] M.O. Abdalla, A. Ludwick, T. Mitchell, Polymer (Guildf). 44 (2003) 7353–7359.

[11] E.S. de Medeiros, J. a M. Agnelli, K. Joseph, L.H. de Carvalho, L.H.C. Mattoso, J. Appl. Polym. Sci. 90 (2003) 1678–1682.

[12] G. He, B. Riedl, A. Aït-Kadi, J. Appl. Polym. Sci. 89 (2003) 1371–1378.

[13] K.P. Singh, G.R. Palmese, J. Appl. Polym. Sci. 91 (2004) 3096–3106.

[14] S. Plimpton, J. Comput. Phys. 117 (1995) 1–19.

[15] W.L. Jorgensen, D.S. Maxwell, J. Tirado-Rives, J. Am. Chem. Soc. 118 (1996) 11225–11236.

[16] W.D. Cornell, P. Cieplak, C.I. Bayly, I.R. Gould, K.M. Merz, D.M. Ferguson, D.C. Spellmeyer, T. Fox, J.W. Caldwell, P.A. Kollman, J. Am. Chem. Soc. 117 (1995) 5179–5197.

[17] B. Hess, C. Kutzner, D. van der Spoel, E. Lindahl, J. Chem. Theory Comput. 4 (2008) 435–447.

[18] D. Kony, W. Damm, S. Stoll, W.F. van Gunsteren, J. Comput. Chem. 23 (2002) 1416–1429.

[19] D.J. Price, C.L. Brooks III, J. Chem. Phys. 121 (2004) 10096–10103.

[20] S. Nose, J. Chem. Phys. 81 (1984) 511–519.

[21] W.G. Hoover, Phys. Rev. A 31 (1985) 1695–1697.

[22] W.G. Hoover, Phys. Rev. A 34 (1986) 2499–2500.

[23] A. Luzar, D. Chandler, J. Chem. Phys. 98 (1993) 8160–8173.

[24] Y. Tamai, H. Tanaka, K. Nakanishi, Macromolecules 29 (1996) 6750–6760.

[25] S.A. Deshmukh, S.K.R.S. Sankaranarayanan, K. Suthar, D.C. Mancini, J. Phys. Chem. B 116 (2012) 2651–2663.

[26] D. Shivakumar, J. Williams, Y. Wu, W. Damm, J. Shelley, W. Sherman, J. Chem. Theory Comput. 6 (2010) 1509–1519.

[27] T.C. Beutler, A.E. Mark, R.C. van Schaik, P.R. Gerber, W.F. van Gunsteren, Chem. Phys. Lett. 222 (1994) 529–539.

[28] D.C. Rapaport, Mol. Phys. 50 (1983) 1151–1162.

[29] M.P. Allen, D.J. Tildesley, Computer Simulation of Liquids, Oxford University Press, New York, 1987.

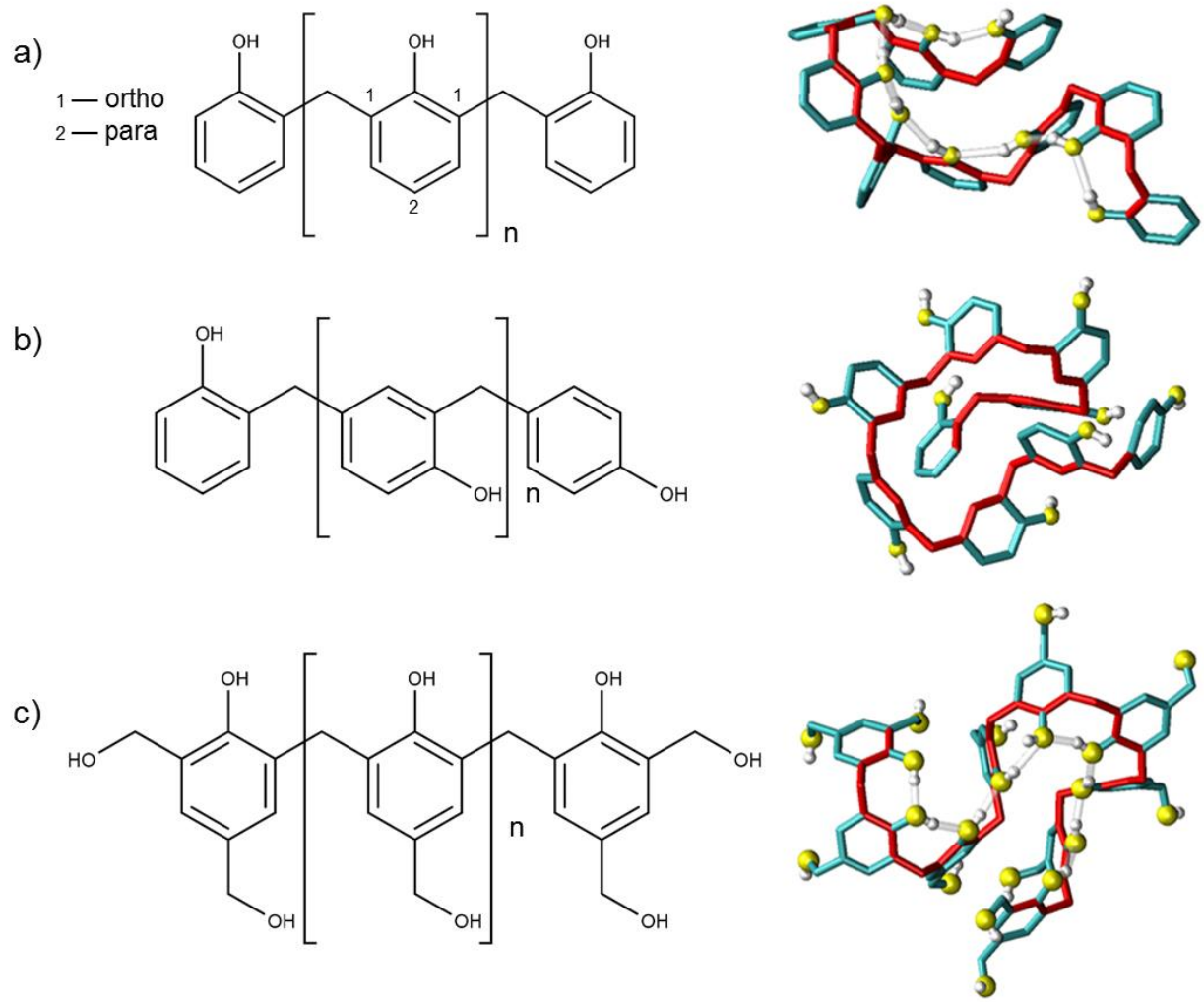

Figure 1. Structures of phenolic chains considered in this study illustrating (a) ortho-ortho repeating novolac-type (*OON*) phenolic chain indicating ortho and para linking sites on a phenol ring, (b) ortho-para repeating novolac-type (*OPN*) phenolic chain, and (c) ortho-ortho repeating resole-type (*RES*) phenolic chain. Images on the right are the corresponding 9-phenol ring chains, and the chains are colored as: carbon backbone (red), non-backbone carbon (cyan), oxygen (yellow), and hydroxyl hydrogen (white). Translucent bonds indicate intramolecular h-bonding. Aromatic and methylene hydrogens are removed for clarity.

Table 1. MD system details.

Chain type	# of phenol rings	# of atoms in chain	# of EGL molecules	# of H_2O molecules
OON	3	41	500	2150
OON	9	125	1700	7900
OPN	9	125	1800	7900
RES	9	169	2100	9000
OON	27	377	21800	90900

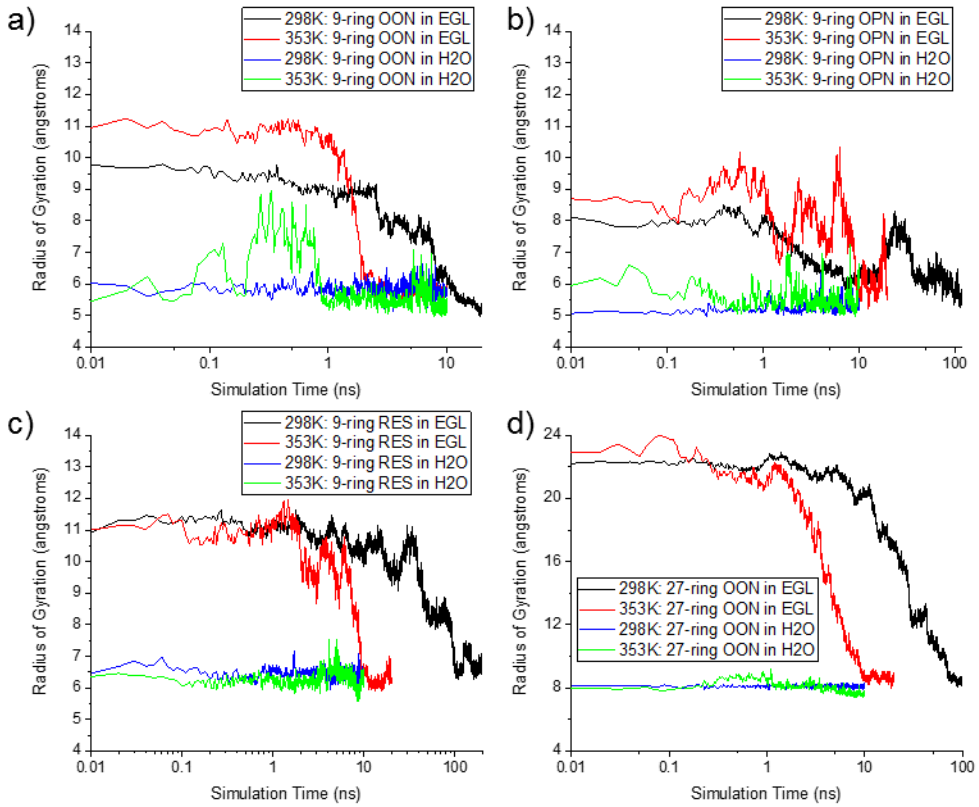

Figure 2. Radius of gyration of phenolic chains in EGL and H_2O at different temperatures for (a) 9-ring OON, (b) 9-ring OPN, (c) 9-ring RES, and (d) 27-ring OON systems. Simulations are run until structures are equilibrated.

Table 2. Free energy (ΔG_{solv}), internal energy (ΔE_{solv}), entropy (ΔS_{solv}) of solvation for different chains and solvents. ΔE_{S-S} is the non-bonded, S-S energy of the solvated polymer relative to the pure solvent. ΔE_{P-P} is the non-bonded P-P energy of the solvated polymer relative to the pure polymer. E_{S-P} is the non-bonded, S-P energy of the solvated polymer. Energy units are kcal/mol and entropy are kcal/mol/K. P and S refer to phenolic and solvent, respectively.

Chain	Solvent	ΔG_{solv}	ΔE_{solv}	ΔS_{solv}	ΔE_{S-S}	ΔE_{P-P}	E_{S-P}
OON	EGL	-27.153	-31.602	-0.015	107.791	7.834	-154.160
OPN	EGL	-53.070	-85.431	-0.109	101.015	11.596	-196.395
RES	EGL	-84.014	-114.016	-0.101	161.575	24.962	-298.565
OON	H_2O	-8.552	-30.606	-0.074	64.320	7.423	-101.015
OPN	H_2O	-23.842	-54.258	-0.102	84.006	10.601	-147.700
RES	H_2O	-46.521	-86.151	-0.133	133.382	20.844	-237.553

Table 3. Energy partitioning analysis of solvated phenolic systems for specified interactions between Solvent element groups and Phenolic element groups. Units for energy are in kcal/mol.

Chain type	Solvent	Solvent OH to Phenolic OH	Solvent OH to Phenolic CH	Solvent CH to Phenolic OH	Solvent CH to Phenolic CH
OON	EGL	-310.613	108.236	248.375	-200.158
OPN	EGL	-332.069	104.964	214.961	-184.251
RES	EGL	-865.171	597.492	649.855	-680.741
OON	H_2O	-69.458	-31.557		
OPN	H_2O	-116.466	-31.234		
RES	H_2O	-229.184	-8.369		

Table 4. Energy partitioning analysis of solvated Phenolic systems for specified interactions between the solute chain and solvent element groups as well as between the solvent molecules and solute element groups. Units for energy are in kcal/mol.

Chain type	Solvent	Phenolic to Solvent OH	Phenolic to Solvent CH	Solvent to Phenolic OH	Solvent to Phenolic CH
OON	EGL	-202.377	48.217	-62.238	-91.922
OPN	EGL	-227.105	30.710	-117.108	-79.287
RES	EGL	-267.679	-30.886	-215.316	-83.249
OON	H_2O	-101.015		-69.458	-31.557
OPN	H_2O	-147.700		-116.466	-31.234
RES	H_2O	-237.553		-229.184	-8.369

Table 5. Energy partitioning analysis of specified interactions between solute atom groups for the phenolic chains in solvated and isolated states.

		Solvated Phenolic			Isolated Phenolic		
Chain	Solvent	OH-OH	OH-CH	CH-CH	OH-OH	OH-CH	CH-CH
OON	EGL	-10.298	-156.007	81.744	-19.626	-152.675	79.906
OPN	EGL	22.722	-132.033	48.000	11.596	-134.414	49.911
RES	EGL	142.025	-503.659	262.474	138.668	-541.927	279.137
OON	H_2O	-7.169	-153.075	76.723	-20.636	-152.083	81.775
OPN	H_2O	20.083	-133.502	50.786	13.630	-137.971	51.107
RES	H_2O	165.783	-556.891	288.852	151.131	-565.749	291.518

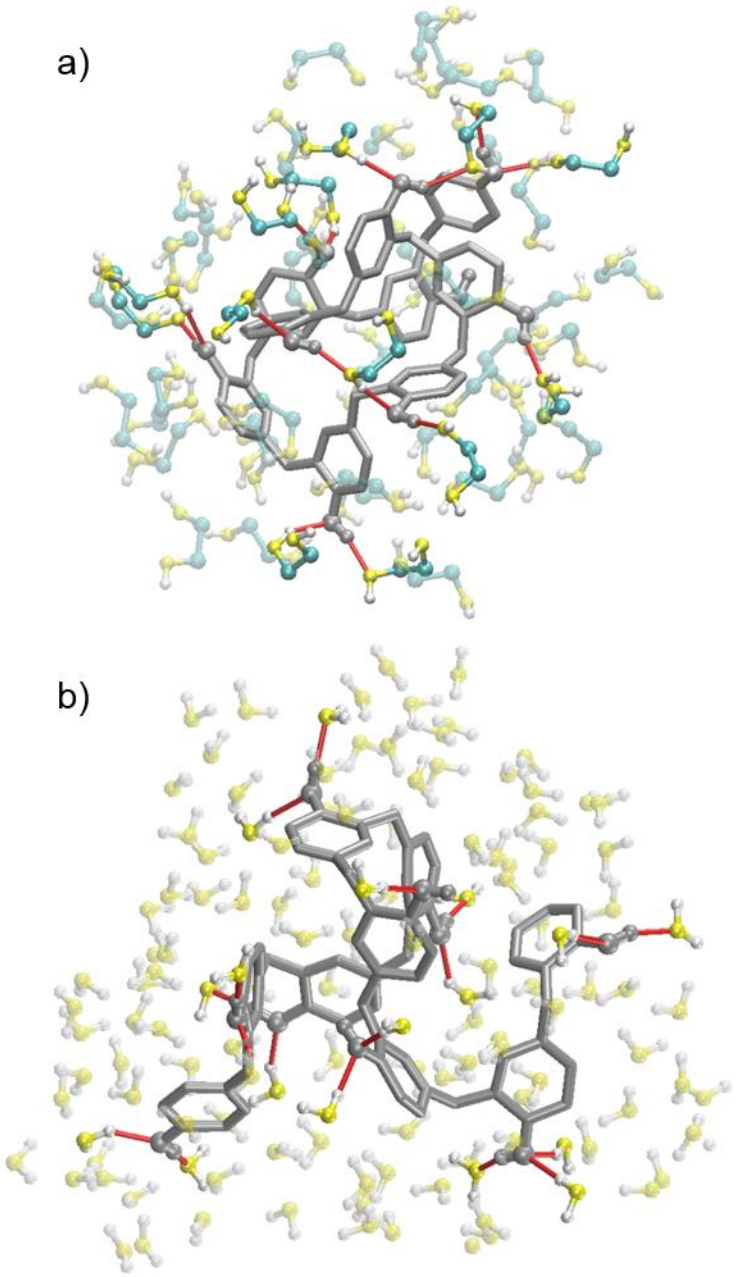

Figure 3. First solvation shell of the OPN chain in a) EGL and b) H_2O solvents. Hydrogen bonds are denoted in red.

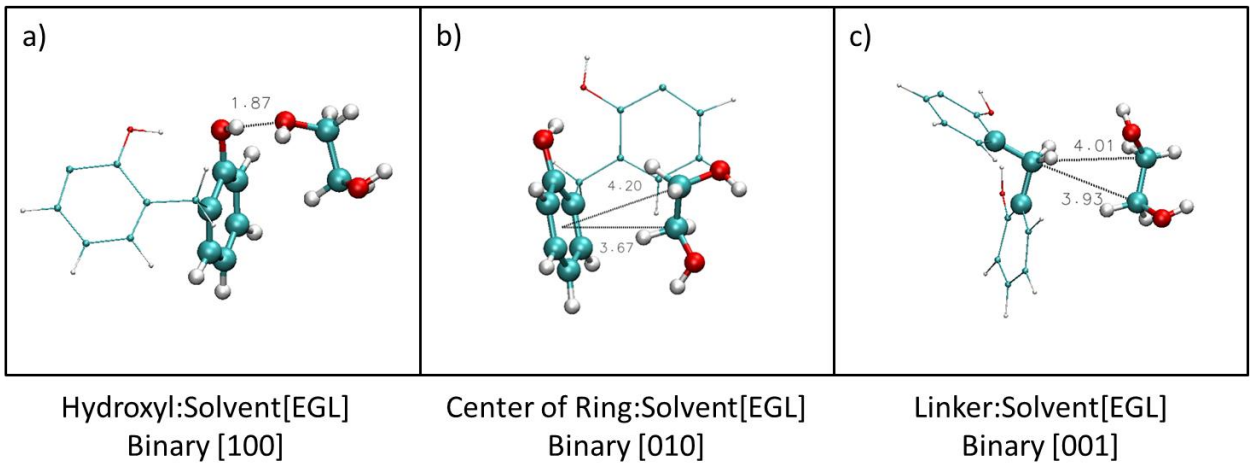

Figure 4. Illustrations of different interaction types between solvent molecules and solute element groups using a binary descriptor (1 = present, 0 = not present); specifically a) phenolic hydroxyl and solvent, denoted [100], b) center of phenolic ring and solvent, denoted [010], and c) phenolic methylene linker and solvent, denoted [001].

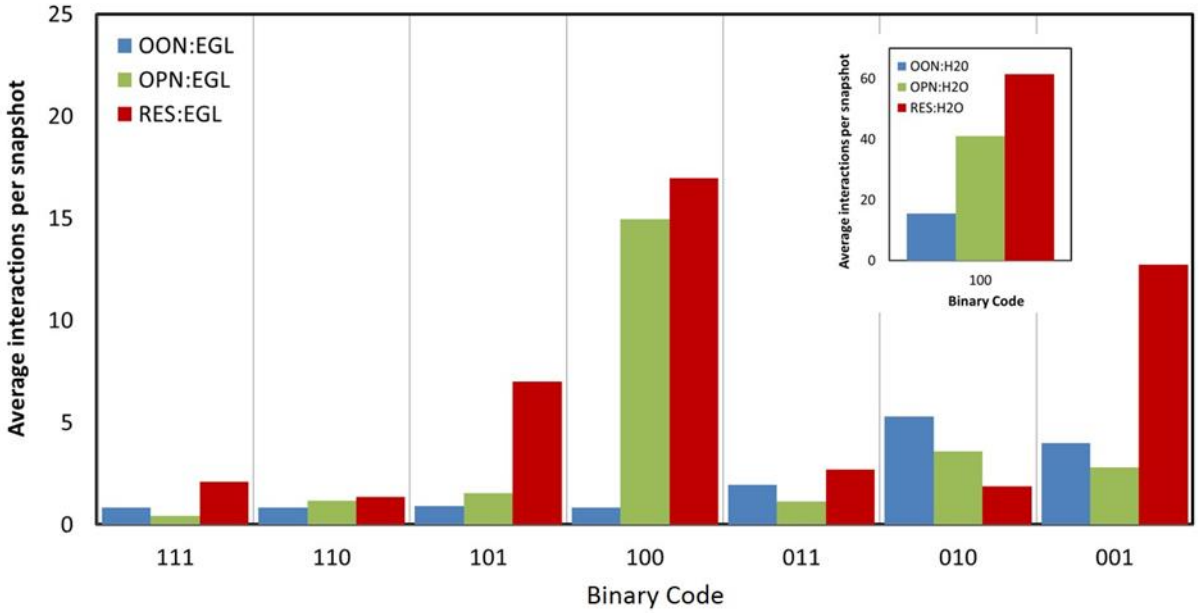

Figure 5. Average number of solvent/phenolic interactions during simulations of phenolic solvated in EGL. Binary code employs naming scheme illustrated in Fig. 4. Inset shows phenolic solvated in H_2O.

Table 6. Average number of hydrogen bonds present during simulations of solvated phenolic chains in EGL. Note: P and S refer to phenolic and solvent OHs, respectively.

Chain type	# of phenol rings	Temperature (K)	Average # of h-bonds		
			P to S	S to P	P to P
OON	3	298	0.961	0.889	1.902
		353	1.102	0.897	1.514
OON	9	298	0.875	1.175	7.129
		353	0.563	1.031	7.097
OPN	9	298	7.353	4.619	0.039
		353	6.006	4.217	0.100
RES	9	298	10.303	10.838	8.017
		353	9.421	9.962	7.670
OON	27	298	0.875	2.584	22.906
		353	1.301	2.276	21.090

Table 7. Average number of hydrogen bonds present during simulations of solvated phenolic chains in H_2O. Note: P and S refer to phenolic and solvent OHs, respectively.

Chain type	# of phenol rings	Temperature (K)	Average # of h-bonds		
			P to S	S to P	P to P
OON	3	298	0.976	2.047	1.801
		353	1.132	1.895	1.446
OON	9	298	1.748	4.389	6.378
		353	1.806	3.557	6.279
OPN	9	298	7.013	9.266	0.054
		353	5.981	7.418	0.084
RES	9	298	9.369	17.897	7.950
		353	8.401	15.002	7.681
OON	27	298	4.495	10.619	18.961
		353	1.549	6.118	21.110

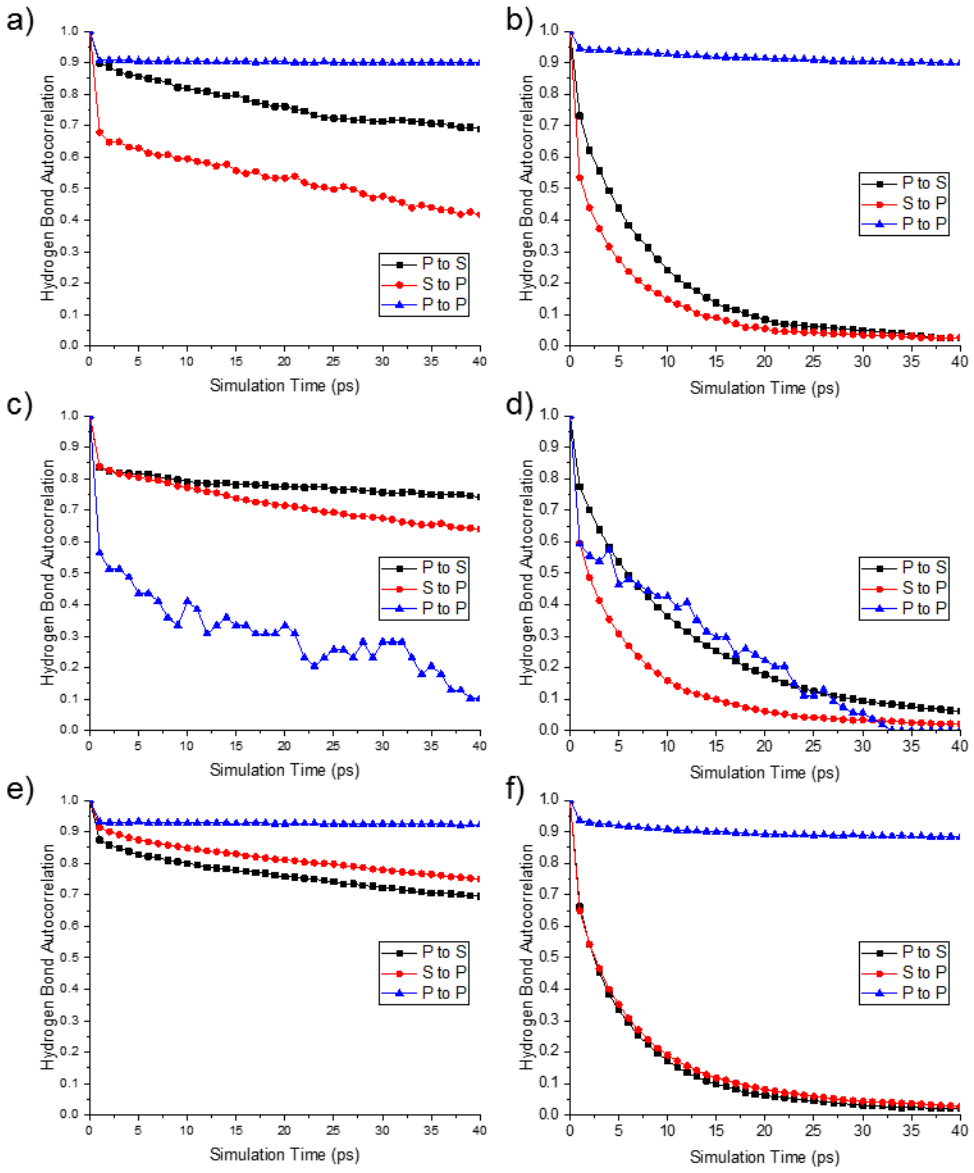

Figure 6. Hydrogen bond autocorrelations using intermittent definition for 9-ring solvated phenolic simulations at 298K. Solvents are EGL [(a),(c),(e)] and H_2O [(b),(d),(f)]. Solutes are OON [(a),(b)], OPN [(c),(d)], and RES [(e),(f)]. Legend notes: P and S refer to phenolic and solvent OHs, respectively.

Table 8. Hydrogen bond residence times determined from exponential fits of the continuous hydrogen bond autocorrelation function for the solvated phenolic chains in EGL. Note: P and S refer to phenolic and solvent OHs, respectively.

Chain type	# of phenol rings	Temperature (K)	H-bonds residence time (ps)		
			P to S	S to P	P to P
OON	3	298	15.777	21.805	33.378
		353	6.795	3.152	10.882
OON	9	298	11.889	5.675	28.324
		353	2.902	2.863	25.670
OPN	9	298	19.765	13.912	2.977
		353	6.827	3.592	1.537
RES	9	298	20.082	25.715	49.400
		353	4.318	5.582	30.253
OON	27	298	7.818	7.162	74.615
		353	4.112	2.952	21.278

Table 9. Hydrogen bond residence times determined from exponential fits of the continuous hydrogen bond autocorrelation function for the solvated phenolic chains in H_2O. Note: P and S refer to phenolic and solvent OHs, respectively.

Chain type	# of phenol rings	Temperature (K)	H-bonds residence time (ps)		
			P to S	S to P	P to P
OON	3	298	5.803	1.589	14.517
		353	2.819	0.882	8.844
OON	9	298	3.810	2.050	22.269
		353	3.243	1.093	13.630
OPN	9	298	5.923	2.284	3.938
		353	2.970	1.220	1.045
RES	9	298	2.969	2.885	25.709
		353	1.606	1.479	15.297
OON	27	298	4.372	2.267	29.158
		353	3.260	1.550	16.120

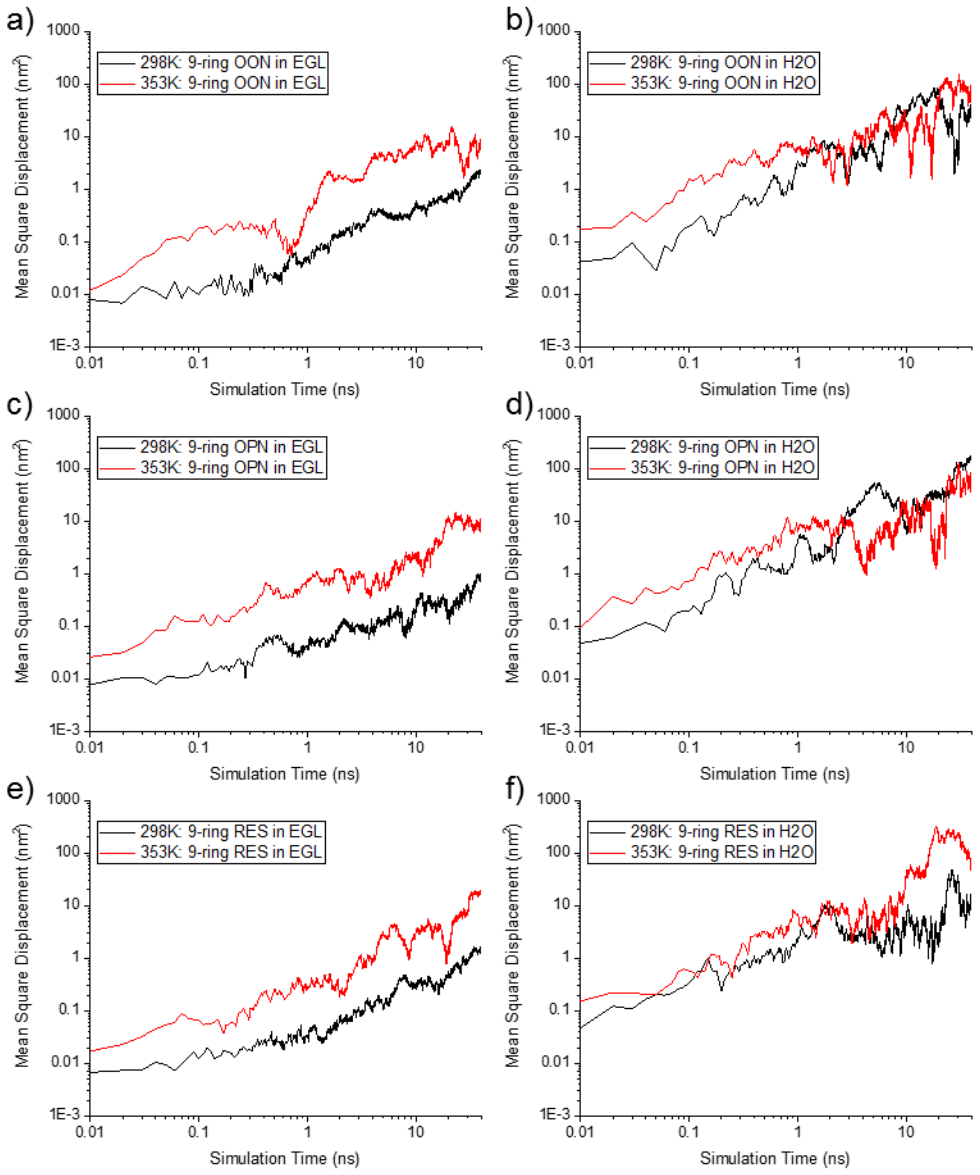

Figure 7. Mean square displacements of the 9-ring phenolic chains in solution. Solvents are EGL [(a),(c),(e)] and H_2O [(b),(d),(f)]. Solutes are OON [(a),(b)], OPN [(c),(d)], and RES [(e),(f)].

Table 10. Diffusion coefficients of the 9-ring phenolic chains in solution.

			Diffusion Coefficient (x10^{10} m^2/s)	
Chain type	Solvent	Temperature (K)	Phenolic	Solvent
OON	EGL	298	0.089 ± 0.006	0.378 ± 0.001
		353	0.293 ± 0.076	4.459 ± 0.016
	H_2O	298	1.155 ± 0.230	41.805 ± 0.122
		353	3.099 ± 0.690	93.738 ± 0.263
OPN	EGL	298	0.037 ± 0.004	0.371 ± 0.001
		353	0.364 ± 0.046	4.536 ± 0.014
	H_2O	298	6.037 ± 0.650	42.208 ± 0.124
		353	2.581 ± 0.558	92.729 ± 0.279
RES	EGL	298	0.062 ± 0.005	0.377 ± 0.001
		353	0.772 ± 0.059	4.369 ± 0.011
	H_2O	298	0.429 ± 0.130	41.450 ± 0.106
		353	3.896 ± 0.874	95.036 ± 0.304